EXPERIMENTAL VERIFICATION OF TEMPERATURE EFFECTS ON FUNCTIONAL PARAMETERS IN A LINE START PERMANENT MAGNET SYNCHRONOUS MOTOR

M. BARANSKI*, W. ŁYSKAWINSKI*, W. SZELAG*, A. DEMENKO*

*Poznan University of Technology, Institute of Industrial Electrical Engineering
Piotrowo 3a, 60-965 Poznań, Poland
{mariusz.baranski/wieslaw.lyskawinki/wojciech.szelag/andrzej.demenko}@put.poznan.pl

Keywords: LSPMSM, temperature impact, Finite Element Method

Abstract

The paper deals with the finite element (FE) analysis of the temperature influence on functional parameters of the line start permanent magnet synchronous motor (LSPMSM). The two-dimensional (2D) FE model of coupled electromagnetic and thermal phenomena in the LSPMSM was described. The nonlinearity of the magnetic circuit and the influence of temperature on the magnetic properties of permanent magnets as well as on the electric and thermal properties of the materials have been considered.The simulation results were validated by measurements of the prototype motor, showing satisfactory concordance.

1 Introduction

In an effort to reduce electric energy consumption, induction motors (IMs) are increasingly being replaced by LSPMSMs [1]. These motors have a much lower energy consumption (higher efficiency and power factor) than IMs. Operation of these motors can take place at various loads and ambient temperatures which causes considerable temperature changes in the components of the motors [2]. The change in temperature affects the properties of permanent magnets and conductive materials, which consequently changes functional parameters of the motors. These parameters can also be affected by the motor's supply voltage, which is determined by voltage drops on the supply grid. Therefore, the authors decided to study the impact of temperature on the functional parameters of LSPMSMs at different supply voltages and loads.

2 Mathematical model of the LSPMSM

The coupled electromagnetic and thermal phenomena model of the LSPMSM contains equations of an electromagnetic field, temperature distributions and motion [2]. After the discretization of time derivatives and using a backward differential scheme, a set of nonlinear algebraic coupled equations describing: the distribution of the magnetic field and currents in the windings (1), the distribution of temperature (2) and angular velocity of the rotor (3) can be written in the following matrix forms:

$$\begin{bmatrix} \boldsymbol{S}^n+\boldsymbol{G}(\boldsymbol{1}-\boldsymbol{Y})\Delta t^{-1} & -\boldsymbol{z} \\ -\boldsymbol{z}^T & -(\boldsymbol{R}\Delta t+\boldsymbol{L}) \end{bmatrix} \begin{bmatrix} \boldsymbol{\varphi}^n \\ \boldsymbol{i}^n \end{bmatrix} = \begin{bmatrix} \boldsymbol{H}_m^n \\ -\Delta t \boldsymbol{U}^n \end{bmatrix} + \begin{bmatrix} \boldsymbol{G}(\boldsymbol{1}-\boldsymbol{Y})\Delta t^{-1} & 0 \\ -\boldsymbol{z}^T & -\boldsymbol{L} \end{bmatrix} \begin{bmatrix} \boldsymbol{\varphi}^{n-1} \\ \boldsymbol{i}^{n-1} \end{bmatrix} \tag{1}$$

$$\left(\boldsymbol{S}_\tau^n+\boldsymbol{K}_{\tau b}^n+\boldsymbol{Y}_\tau^n\Delta t^{-1}\right)\boldsymbol{\tau}^n=\boldsymbol{Q}^n+\boldsymbol{K}_{\tau o}^n+\boldsymbol{Y}_\tau^n\Delta t^{-1}\boldsymbol{\tau}^{n-1} \tag{2}$$

$$J_i\left(y^{n+1}-2y^n+y^{n-1}\right)/(\Delta t)^2=T^n-T_L^n \tag{3}$$

where $\boldsymbol{U}$ is the vector of supply voltages; $\boldsymbol{i}$ is the vector of loop currents; $\boldsymbol{\varphi}$ is the vector of edge values of magnetic vector potentials; $\boldsymbol{\tau}$ is the vector of nodal values of temperature; $\boldsymbol{Y}$, $\boldsymbol{G}$, $\boldsymbol{R}$, $\boldsymbol{L}$, $\boldsymbol{S}_\tau$, $\boldsymbol{K}_{\tau b}$ $\boldsymbol{Y}_\tau$, $\boldsymbol{P}$, $\boldsymbol{K}_{\tau o}$, arethe matrices of coefficients; $\boldsymbol{z}$ is the matrix describing the number of turns assigned to the mesh nodes, J_i is the moment of inertia; γ is the angular position of the rotor; T_L is the load torque; T is the electromagnetic torque calculated using $\boldsymbol{\varphi}$; Δt is the time step length. In the considered coupled problems, the elements of the matrix of resistances $\boldsymbol{R}$, the matrix of conductances $\boldsymbol{G}$ and the matrix of thermal conductivities $\boldsymbol{S}_\tau$ depend on temperature. The entries of the magnetization vector $\boldsymbol{H}_m$ are calculated accordingly to families of demagnetization characteristics and interpolation techniques in relation to magnetic flux density, magnetic field, and temperature. The presented system of non-linear equations (1)-(3) is solved for each time step simultaneously using the block relaxation method [2].

3 Results

The authors used their own software to analyse the effect of temperature on the functional parameters of the LSPMSM. The in-house developed code takes into consideration the temperature impact on magnetic, electrical and thermal properties of electromagnetically active materials and has been used to study the influence of temperature on functional parameters in LSPMSMs. The geometry of the considered 3-phase, 4-pole, 3.4-kW output power, 1500-rpm LSPMSM is shown in Fig. 1. The simulation results have been compared with the results of the measurement tests. The laboratory stand to measure the functional parameters of LSPMSMs working in higher temperatures is shown in Fig. 2. The tested motor was placed in a heating chamber and was loaded by a magnetorheological fluid (MRF) brake. The tests were carried out for selected temperatures of fixed components of the motor, i.e. $\tau = 40\,^0$C and $\tau = 100\,^0$C. The measurements were made after the temperature of the motor components was established.

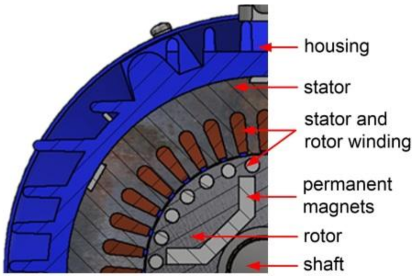

Fig. 1: Geometry of the field model of LSPMSM

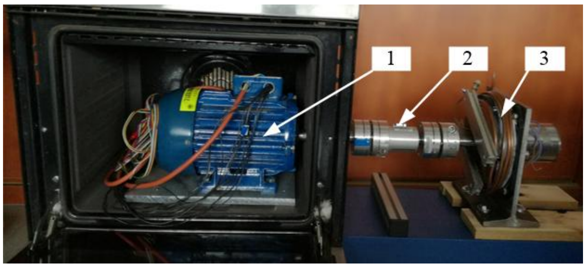

Fig.2: Laboratory stand: 1 – LSPMSM, 2 – torque transducer, 3 – MRF brake

The temperature impact on the selected functional parameters in LSPMSMs was studied. The influence of the supply voltage on the phase current I_{ph} (Fig. 3a), efficiency η (Fig. 3b) as well as power factor $cos\varphi$ (Fig. 3c) of motor working in low and high temperatures has been examined.

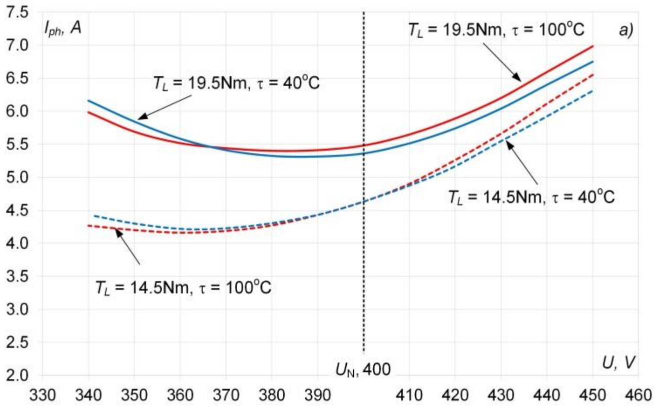

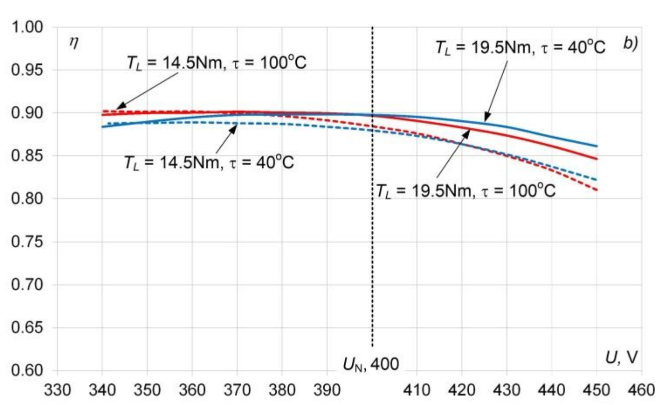

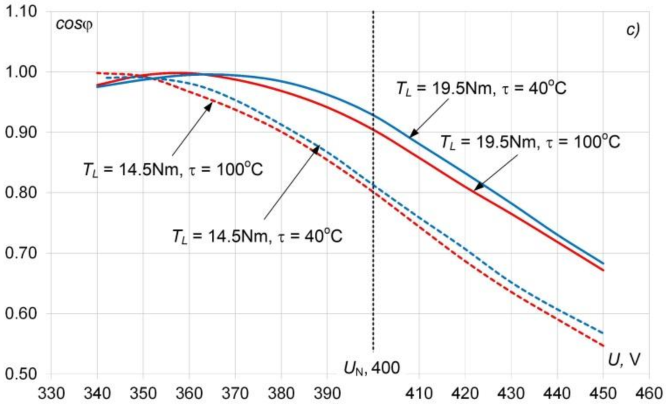

Fig.3a-c. Measured phase current (a), efficiency (b) and power factor (c) v.s. supply voltage for T_L =19.5 Nm, T_L =14.5 Nm and τ = 40 ^{0}C, τ = 100 ^{0}C

The simulations have been performed for supply voltage from 340 V to 450 V for two values of load torque, i.e. T_L = 19.5 Nm and T_L =14.5 Nm. The measured and calculated values of I_{ph}, η and $cos\varphi$ obtained for T_L = 19.5 Nm, T_L =14.5 Nm and τ = 40 ^{0}C and τ = 100 ^{0}C in an electromechanical and thermal steady-state condition at U_N=400V are summarized in Table 1.

T_L [Nm]	Calculated						Measured					
	τ = 40 ^{0}C			τ = 100 ^{0}C			τ = 40 ^{0}C			τ = 100 ^{0}C		
	I_{ph} [A]	η [-]	$cos\varphi$ [-]	I_{ph} [A]	η [-]	$cos\varphi$ [-]	I_{ph} [A]	η [-]	$cos\varphi$ [-]	I_{ph} [A]	η [-]	$cos\varphi$ [-]
14.5	4.50	0.869	0.800	4.60	0.878	0.801	4.54	0.880	0.819	4.63	0.884	0.801
19.5	5.33	0.875	0.902	5.57	0.892	0.904	5.36	0.898	0.928	5.58	0.897	0.904

Table 1: Selected functional parameters at U_N=400V

4 Conclusions

Based on the simulation and measurement results, it can be concluded that the proposed model and developed software provide satisfactory accuracy. The performed tests confirmed that the optimal functional parameters were obtained at a supply voltage between 360 V and 380 V. For such supply voltages, the analyzed motor draws the lowest current while the value of the product of efficiency and power factor is the highest. A detailed comparison of the calculation and measurement results will be discussed during the upcoming conference and presented in the full version of the paper.

References

[1] A. U. Ganesan and L. N. Chokkalingam, "Review on the evolution of technology advancements and applications of line-start synchronous machines", *IET Electric Power Applications*, **13(1)**, pp. 1–16, (2019)

[2] M. Baranski, W. Szelag, and W. Lyskawinski, "Experimental and Simulation Studies of Partial Demagnetization Process of Permanent Magnets in Electric Motors", *IEEE Transactions on Energy Conversion*, **36(4)**, pp. 3137–3145, (2021)